Journal of Neuropathology & Experimental Neurology, 2024, **83**, 194–204
https://doi.org/10.1093/jnen/nlad102
Advance access publication 16 January 2024
Original Article

YTHDF2-regulated matrilin-3 mitigates post-reperfusion hemorrhagic transformation in ischemic stroke via the PI3K/AKT pathway

Hanze Chen, PhD[1], Siping Guo, MD[2], Runnan Li, MD[2], Lihui Yang, MD[2], Rui Wang, MD[2], Yasi Jiang, PhD[2], Yonggang Hao, PhD[1,2,*]

[1]Department of Neurology, Sir Run Run Shaw Hospital, Zhejiang University School of Medicine, Hangzhou City, Zhejiang Province, China
[2]Department of Neurology, Dushu Lake Hospital Affiliated to Soochow University, Suzhou City, Jiangsu Province, China

*Send correspondence to: Yonggang Hao, PhD, Department of Neurology, Dushu Lake Hospital Affiliated to Soochow University, No. 9 Chongwen Road, Industrial Park, Suzhou City, Jiangsu Province 215000, China; Sir Run Run Shaw Hospital, Zhejiang University School of Medicine, 3 Qingchun East Road, Hangzhou City, Zhejiang Province 310000, China; E-mail: heyongg_hyg@163.com
Hanze Chen and Siping Guo contributed equally to this work.

ABSTRACT

Hemorrhagic transformation can complicate ischemic strokes after recanalization treatment within a time window that requires early intervention. To determine potential therapeutic effects of matrilin-3, rat cerebral ischemia-reperfusion was produced using transient middle cerebral artery occlusion (tMCAO); intracranial hemorrhage and infarct volumes were assayed through hemoglobin determination and 2,3,5-triphenyltetrazoliumchloride (TTC) staining, respectively. Oxygen-glucose deprivation (OGD) modeling of ischemia was performed on C8-D1A cells. Interactions between matrilin-3 and YTH N6-methyladenosine RNA binding protein F2 (YTHDF2) were determined using RNA immunoprecipitation assay and actinomycin D treatment. Reperfusion after tMCAO modeling increased hemorrhage, hemoglobin content, and infarct volumes; these were alleviated by matrilin treatment. Matrilin-3 was expressed at low levels and YTHDF2 was expressed at high levels in ischemic brains. In OGD-induced cells, matrilin-3 was negatively regulated by YTHDF2. Matrilin-3 overexpression downregulated p-PI3K/PI3K, p-AKT/AKT, ZO-1, VE-cadherin and occludin, and upregulated p-JNK/JNK in ischemic rat brains; these effects were reversed by LY294002 (a PI3K inhibitor). YTHDF2 knockdown inactivated the PI3K/AKT pathway, inhibited inflammation and decreased blood-brain barrier-related protein levels in cells; these effects were reversed by matrilin-3 deficiency. These results indicate that YTHDF2-regulated matrilin-3 protected ischemic rats against post-reperfusion hemorrhagic transformation via the PI3K/AKT pathway and that matrilin may have therapeutic potential in ischemic stroke.

KEYWORDS: Blood-brain barrier, Hemorrhagic transformation, Ischemic stroke, Matrilin-3, PI3K/AKT signaling pathway, YTH N6-methyladenosine RNA binding protein F2

INTRODUCTION

Stroke is an acute cerebrovascular disease caused by obstruction of cerebral blood circulation, principally resulting in ischemic infarction and intracerebral hemorrhage (1). Ischemic strokes account for 80% of all strokes and are the consequence of a local disruption of blood supply to the brain tissues that lead to hypoxia and necrosis, which in turn result in a range of neurological impairments (2, 3). Current effective treatments for acute ischemic stroke include intravenous thrombolysis and mechanical thrombectomy (4–6). However, hemorrhagic transformation is a major complication of acute cerebral infarct recanalization and it is correlated with mortality and poor patient outcome. A recent study pointed out that only one-third of patients with hemorrhagic transformation had a good prognosis compared to those without hemorrhage and the mortality rate was 5 times higher (7). Therefore, early identification or prediction of risk factors for intracranial hemorrhage after intravascular treatment is of great significance for guiding clinical practice.

Available studies have suggest that intracranial hemorrhage after recanalization therapy is correlated with endothelial and basement membrane damage, increased blood-brain barrier (BBB) permeability, reperfusion injury-induced inflammatory responses and oxidative stress (8, 9). The phosphoinositide 3-kinase/protein kinase B (PI3K/AKT) pathway is widely present in various neural cells and is a vital pathway for intracellular transduction of membrane receptor signals that regulate cell proliferation, differentiation, metabolism, antiapoptosis, and other biological functions (10). Available studies have demonstrated that intervention with the PI3K/AKT

pathway can notably promote or inhibit the expressions of related factors, thereby reducing neuronal apoptosis and exerting neuroprotective effects in treatments for ischemic stroke, spinal cord injury, and epilepsy (11–13). Finding effective targets for regulating this signaling pathway is critical for preventing neurological damage after ischemic stroke and reducing the risk of hemorrhagic transformation.

Matrilins are a group of noncollagenous extracellular adaptor proteins that are expressed in cartilage, as well as many other extracellular matrices (ECMs). They are involved in the assembly and stabilization of the ECM through protein-to-protein interactions, largely due to their von Willebrand factor A-like domains (14). Recent studies have verified that matrilin is expressed in neurons, astrocytes, and different brain regions, contributing to the repair and stabilization of the BBB (15–17). New evidence from genome-wide association studies has suggested that the alteration of matrilin-3 is associated with the development of neurological diseases (18). Currently, matrilin-3 is frequently reported to play a chondroprotective role through the regulation of anti-inflammatory functions and ECM components, which might be related to the PI3K/AKT pathway (19–21). According to the previous analysis of matrilin-3 distribution in brain tissues using ScRNASeqDB database (https://bioinfo.uth.edu/scrnaseqdb/), we find that matrilin-3 is mainly distributed in astrocytes and endothelial cells. However, little is known about the effect of matrilin-3 on ischemic strokes.

The present study was designed to explore the underlying mechanism of matrilin-3 effects on hemorrhagic transformation after reperfusion in ischemic stroke with the aim to provide a new scheme to prevent hemorrhagic transformation following acute ischemic stroke.

MATERIALS AND METHODS

Animals

Sprague-Dawley rats (male, 250–290 g, Charles River, Beijing, China) were used in this study. The rats were housed at a constant temperature (25 ± 2°C) and a consistent light/dark cycle (12 hour/12 hour) with available food and drinking water. All procedures in animal experiments were approved by the Committee of Laboratory Animals of Sir Run Shaw Hospital (ISHT20200622), and carried out in strict accordance with the guideline from the Care and Use of Laboratory Animals.

PI3K inhibition

LY294002 (HY-10108), as a PI3K inhibitor, was purchased from MedChemExpress (Monmouth Junction, NJ) and then diluted to 0.5 mg/mL in dimethyl sulfoxide (D103277, Aladdin, Shanghai, China). Rats were injected with LY294002 solution (10 μL) via the tail vein 1 hour before the performance of transient middle cerebral artery occlusion (tMCAO) (22).

Construction of adenoviral plasmid

To induce in vivo matrilin-3 overexpression, rat complementary DNA (cDNA) for matrilin-3 was inserted into adenoviral shuttle vector pDC316-mCMV-EGFP (HG-VXY0585, HonorGene, Changsha, China) to yield mCMV-matrilin-3-EGFP plasmid which was then co-transfected with adenoviral backbone plasmid [pBHGlox(delta)E1,3Cre] (VT2214, Youbio, Changsha, China) into HEK-293 cells according to the instructions of AdMax packaging system (23). After amplification, the purified adenovirus (Adv) were subjected to virus titer detection using Adeno-X-Rapid Titer-Kit (632250, Takara, Tokyo, Japan). Adv-EGFP with empty coding sequences for matrilin-3 was used as the negative control.

Rat modeling and treatment

After acclimation, rats were randomly divided into the following groups (n = 5 rats/group): Control, tMCAO (2 hours of tMCAO and reperfusion), tMCAO+NC (2 hours of tMCAO and reperfusion, and Adv-EGFP injection), tMCAO+Matrilin-3 (2 hours of tMCAO and reperfusion, and Adv-matrilin-3 injection), and tMCAO+Matrilin-3 + LY294002 groups (2 hours of tMCAO and reperfusion, Adv-matrilin-3 and LY294002 injection). To investigate the mechanism of matrilin-3 in hemorrhagic transformation after ischemic stroke, we established tMCAO in rat as previously described (24). In short, the right common carotid artery (CCA), internal carotid artery, and external carotid artery (ECA) were surgically exposed and separated amid rat anesthesia (2%–3% isoflurane, PHR2874, Sigma-Aldrich, St Louis, MO). Then, a nylon suture (0.38 mm in diameter) was inserted into the lumen of ECA until the suture blunted distal end met resistance. Then, 2 hours of occlusion later, the suture was withdrawn to achieve reperfusion. Identical surgical procedures were conducted on rats in the Control group aside for tMCAO. Adv-matrilin-3 or Adv-EGFP (4×10^9 IFU/mL) were injected into the right lateral ventricle of rats through stereotactic catheter per day for 5 days starting from 2 days before ischemia modeling. After 24 hours of treatment, all rats were killed by deep anesthesia (150 mg/kg pentobarbital sodium, P-010, Sigma-Aldrich) combined with cervical dislocation to collect brain samples.

Hemoglobin determination

To evaluate the severity of cerebral hemorrhage, we measured hemoglobin levels in rats as previously described (24). The fresh brain samples were homogenized with cold phosphate-buffered solution ([PBS], abs9459, Absin, Shanghai, China) and then centrifuged (15 000 g) for 15 minutes. Following supernatant collection, Hemoglobin Assay Kit (MAK115, Sigma-Aldrich) was used to detect the content of hemoglobin according to the manufacturer's instructions. The absorbance at 400 nm (A_{400}) was measured using a microplate reader (LogPhase 600, BioTek, Winooski, VT). Concentration of hemoglobin=[(A_{400} sample)−(A_{400} blank)]/[(A_{400} calibrator)−(A_{400} blank)]×100 mg/dL×df, 100 mg/dL=concentration of the diluted calibrator, df=dilution factor (e.g. 100 for the blood samples).

Cell culture and treatment

Mouse type I astrocytes C8-D1A (CRL-2541) were provided by American Type Culture Collection (Manassas, VA) and grown in complete culture medium (CM-M157, Procell, Wuhan, China) a 5% CO_2 incubator at 37°C. For cell

treatment, C8-D1A cells in the glucose-free medium were incubated in normoxic condition (21% O_2, 5% CO_2) and hypoxic condition (0.1% O_2, 5% CO_2, 95% N_2), respectively, for 3, 6, 9, and 12 hours (25).

Short hairpin RNA and cell transfection

To induce in vitro YTH N6-methyladenosine RNA binding protein F2 (YTHDF2) and matrilin-3 knockdown, short hairpin RNA (shRNA) targeting YTHDF2 (shYTHDF2; sense: 5′-GGCUAAUGUGUUUGUUAAAGG-3′, antisense: 5′-UUUAACAAACACAUUAGCCAA-3′), shMatrilin-3 (sense: 5′-GGAGGAUCUUGUUCUAGAACC-3′, antisense: 5′-UUCUAGAACAAGAUCCUCCCU-3′) as well as scramble shRNA were synthesized by GenePharma (Shanghai, China). Next, transfection with shRNA was performed using Lipofectamine 3000 Reagent (L3000075, Thermo Fisher, Waltham, MA) at 37°C for 48 hours when cell confluence reached over 70% in each well of 96-well plates.

RNA immunoprecipitation assay

The binding of YTHDF2 and matrilin-3 was detected using Imprint RIP assay Kit (RIP-12RXN, Sigma-Aldrich). Briefly, 1×10^7 cross-linked cells with shNC or shYTHDF2 were homogenized in Lysis Buffer supplemented with Protease Inhibitor Cocktail. The lysates were incubated with anti-YTHDF2 antibody (MA5-47011, Thermo Fisher, Waltham, MA) or anti-mouse IgG antibody at 4°C overnight, followed by coupling with Protein A Magnetic Beads for 1 hour. Thereafter, the purified RNA samples were determined by qPCR analysis.

RNA decay assay

Actinomycin D (ACTD; SBR00013-1, Sigma-Aldrich) was diluted in the culture medium at a final concentration of 5 μg/mL (26). The cells with shNC or shYTHDF2 were incubated with ACTD for 0, 1, 2, and 3 hours at 37°C, followed by quantitative real-time reverse transcription polymerase chain reaction (qRT-PCR).

RNA extraction and qRT-PCR

Total RNA was extracted from fresh brain tissues and cells using TRIzol reagent (9810, Takara, Japan) and then reversely transcribed into cDNA by Transcriptor First Strand cDNA Synthesis Kit (04379012001, Roche, Switzerland). The amplification of cDNA was conducted on a DNA thermal cycler (ABI 7500, Thermo Fisher) equipped with Fast SYBR Green Master Mix (4385612, Thermo Fisher). The reaction conditions were set as: hold cycle at 95°C for 20 seconds; 40 cycles at 95°C for 10 seconds; extension at 60°C for 30 seconds. GAPDH served as the endogenous control and relative expressions were normalized based on the $2^{-\Delta\Delta Ct}$ method (27). Primer sequences used in qRT-PCR are listed as follows (5′–3′): matrilin-3 (rat: forward: 5′-AAGGTCAGCTCCCATCTCCA-3′, reverse: 5′-ACGGCCATGGCATTTTGTTTAT-3′; mouse: forward: 5′-TCTCCCGCATCATCGACACT-3′, reverse: 5′-GTCGGAATAGGTGTTGAGCTG-3′), YTHDF2 (mouse: forward: 5′-GAGCAGAGACCAAAAGGTCAAG-3′, reverse: 5′-CTGTGGGCTCAAGTAAGGTTC-3′), TNF-α (mouse: forward: 5′-CCCTCACACTCAGATCATCTTCT-3′, reverse: 5′-GCTACGACGTGGGCTACAG-3′), IL-6 (mouse: forward: 5′-TAGTCCTTCCTACCCCAATTTCC-3′, reverse: 5′-TTGGTCCTTAGCCACTCCTTC-3′), and GAPDH (rat: forward: 5′-TAATGCCGCCCCTTACCATC-3′, reverse: 5′-GGTGCAGCGATGCTTTACTT-3′; mouse: forward: 5′-AGGTCGGTGTGAACGGATTTG-3′, reverse: 5′-TGTAGACCATGTAGTTGAGGTCA-3′).

2,3,5-Triphenyltetrazoliumchloride staining

The infract volumes in tMCAO rat brains were visualized by 2,3,5-triphenyltetrazoliumchloride (TTC) staining (28). The brain samples were sliced into 5-μm sections and immersed in TTC solution (17779, Sigma-Aldrich) at 37°C for 30 minutes away from light. Lastly, the stained sections were washed with PBS and fixed with 4% paraformaldehyde (abs9179, Absin, China). Infarct areas were visualized and quantified using Image J Software (vision 1.8.0, National Institutes of Health, Bethesda, MD). Infarct volume=[total infarct volume−(volume of intact ipsilateral hemisphere−volume of intact contralateral hemisphere)]/contralateral hemisphere volume.

Western blot

To reveal the molecular mechanism of matrilin-3 in hemorrhagic transformation, we employed Western blot to detect important protein levels related to PI3K/AKT signaling pathway and BBB (29). Fresh brain tissues or cells were homogenized in RIPA Lysis Buffer (P0013B, Beyotime, China), and the extracted protein was determined with the application of BCA Protein Concentration Assay Kit (E-BC-K318-M, Elabscience, Wuhan, China). Then, each amount of protein was separated by 10% sodium dodecyl sulfate-polyacrylamide gel electrophoresis and loaded onto polyvinylidene fluoride membranes (Millipore, Billerica, MA). After being blocked by 5% skim milk, the membranes were firstly incubated with primary antibodies (Abcam, Cambridge, United Kingdom) against phosphorylated (p)-PI3K (ab182651, 1:500, 84 kDa, Abcam, United Kingdom), PI3K (ab191606, 1:1000, 85 kDa, Abcam, United Kingdom), p-AKT (ab38449, 1:500, 56 kDa, Abcam, United Kingdom), AKT (ab8805, 1:500, 55 kDa, Abcam, United Kingdom), p-JNK (ab76572, 1:5000, 54/46 kDa, Abcam, United Kingdom), JNK (ab179461, 1:1000, 54/46 kDa, Abcam, United Kingdom), ZO-1 (ab190085, 1:500, 195 kDa, Abcam, United Kingdom), VE-cadherin (ab119785, 1:1000, 140 kDa, Abcam, United Kingdom), occludin (ab167161, 1:1000, 59 kDa, Abcam, United Kingdom), YTHDF2 (ab220163, 1:1000, 62 kDa, Abcam, United Kingdom), matrilin-3 (PA5-121125, 1:1000, 53 kDa,), and GAPDH (ab8245, 1:500, 36 kDa Thermo Fisher) at 4°C overnight, and then reacted with secondary antibodies anti-rabbit IgG (ab205718, 1:2000) and anti-mouse IgG (ab6728, 1/2000) (Abcam, United Kingdom) at room temperature for 1 hour. GAPDH served as the internal control. Lastly, immunoblots were probed with ECL Substrate Detection Kit

(E-BC-R347, Elabscience, China) and analyzed using a Tanon 5200 multi automatic chemiluminescence/fluorescence image analysis system (Tanon, Shanghai, China).

Statistical analysis

Statistical analysis was carried out using GraphPad Prism 8.0 (GraphPad Software Inc., San Diego, CA), with measurement data expressed as mean±SD. Statistical differences among multiple groups were compared with 1-way analysis of variance, as well as between 2 independent groups were compared with independent samples t-test. A p-value <0.05 was perceived as statistically significant.

RESULTS

Matrilin-3 reduced hemorrhage and hemoglobin content in ischemic rat brains

We first constructed ischemia-reperfusion injury in the brains of rats that were injected with or without Adv-matrilin-3 to explore the effect of matrilin-3 on hemorrhagic transformation. In accordance with rat brains collected in Figure 1A, we observed a severe hemorrhage in rats of the tMCAO group compared to those of the Control group. This situation was evidently attenuated in the presence of matrilin-3. The results of hemoglobin determination indicated that hemoglobin level was markedly elevated in rats of the tMCAO group (Fig. 1B,

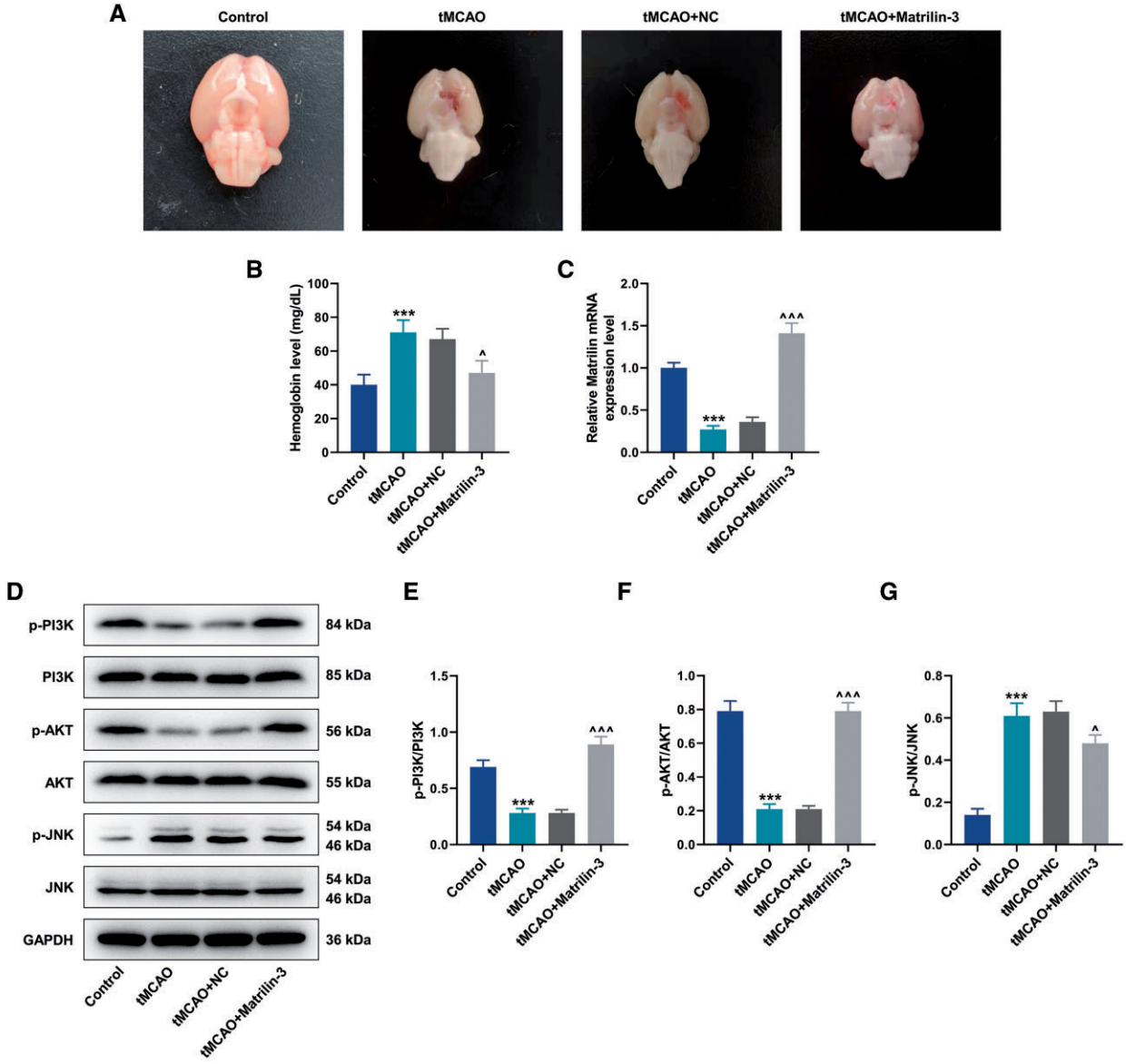

Figure 1. Effects of matrilin-3 on hemorrhagic transformation in ischemic rat brains. **(A)** Ischemic stroke modeling was performed on rats injected with or without adenovirus-mediated matrilin-3 plasmids (Control, tMCAO, tMCAO+NC, and tMCAO+Matrilin-3 groups). Cerebral hemorrhage in rats from each group was observed. **(B)** Hemoglobin level was determined in each group to evaluate the severity of cerebral hemorrhage. **(C)** qRT-PCR was employed to detect the expression of matrilin-3 in each group. **(D–G)** Western blot was used to analyze expressions of p-PI3K/PI3K, p-AKT/AKT, and p-JNK/JNK in each group. GAPDH served as the loading control. The data are presented as the mean±SD of 3 independent experiments; ***$p < 0.001$ versus Control; ^$p < 0.05$, ^^^$p < 0.001$ versus tMCAO+NC. Abbreviations: qRT-PCR, quantitative real-time reverse transcription polymerase chain reaction; PI3K, phosphatidylinositol-3-kinase; p-PI3K, phosphorylated PI3K; AKT, protein kinase B; JNK, c-Jun NH2-terminal kinase; NC, negative control.

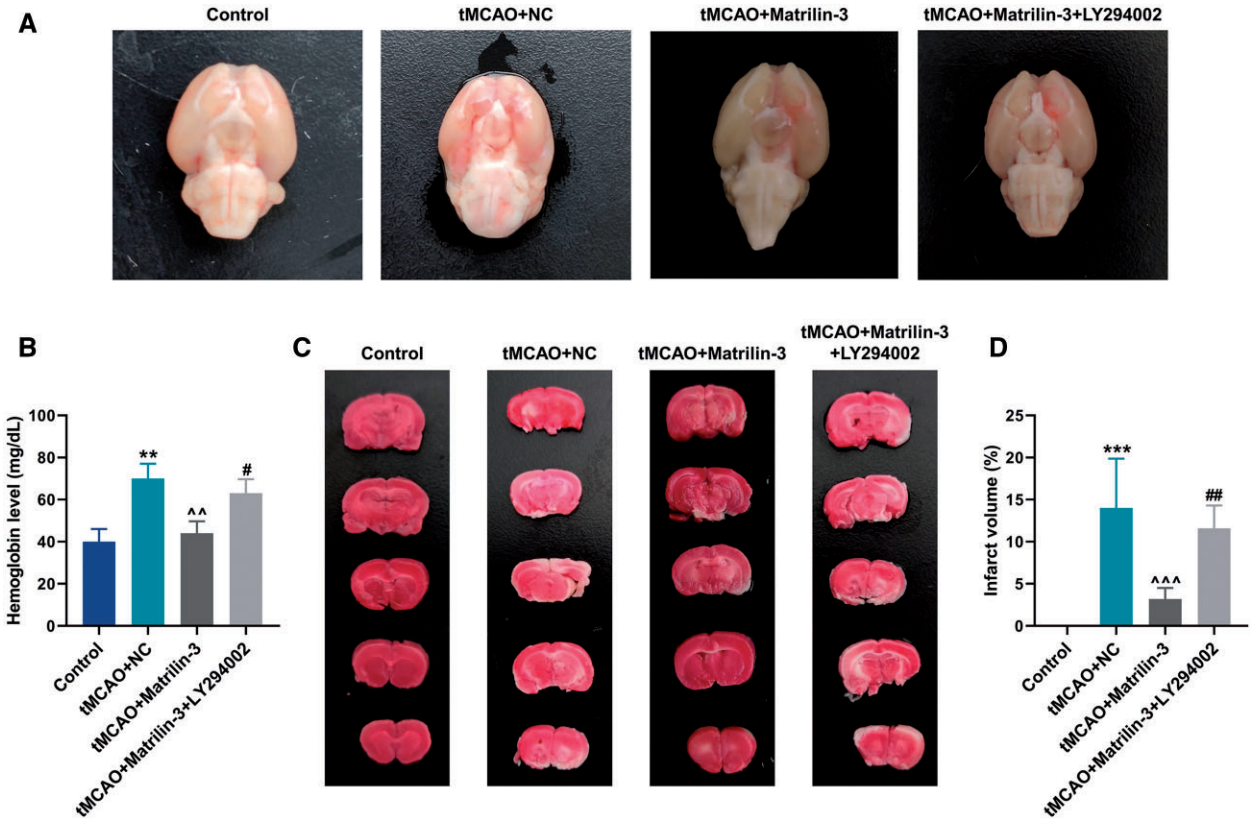

Figure 2. PI3K inhibition reversed the protective role of matrilin-3 in hemorrhagic transformation and infarction in rat brains after tMCAO. **(A)** Ischemic stroke modeling was performed on rats who were injected with or without adenovirus-mediated matrilin-3 plasmids and LY294002 (Control, tMCAO, tMCAO+NC, tMCAO+Matrilin-3, and tMCAO+Matrilin-3 + LY294002 groups). Rat brain sample in each group were collected to observe cerebral hemorrhage. **(B)** Hemoglobin level was determined in each group to evaluate the severity of cerebral hemorrhage. **(C, D)** The infarction area in the TTC-stained brain sections in each group was investigated by observation and quantitative analysis. The data are presented as the mean±SD of 3 independent experiments; $^{**}p < 0.01$, $^{***}p < 0.001$ versus Control; $^{\wedge\wedge}p < 0.01$, $^{\wedge\wedge\wedge}p < 0.001$ versus tMCAO+NC; $^{\#}p < 0.05$, $^{\#\#}p < 0.01$ versus tMCAO+Matrilin-3. Abbreviation: TTC, 2,3,5-triphenyltetrazoliumchloride.

$p < 0.001$). Matrilin-3 overexpression reduced the level of hemoglobin in brains of ischemic rats (Fig. 1B, $p < 0.05$).

Upregulation of matrilin-3 activated PI3K/AKT signaling pathway and inhibited JNK signaling pathway

Low expression of matrilin-3 was found in the brains of rats with ischemia-reperfusion (Fig. 1C, $p < 0.001$); the expression of matrilin-3 was upregulated in brains of ischemic rats following injection with Adv-matrilin-3 (Fig. 1C, $p < 0.001$). Based on previous reports that PI3K/AKT and JNK signaling pathways differently participated in the regulatory mechanism of matrilin in cells (19, 30), we carried out Western blot to detect the protein levels of related markers. Interestingly, decreased expressions of p-PI3K/PI3K and p-AKT/AKT as well as the increased expression of p-JNK/JNK were demonstrated in the tMCAO group (Fig. 1D–G, $p < 0.001$), however, these tendencies were rescued in the tMCAO+Matrilin-3 group (Fig. 1D–G, $p < 0.05$).

PI3K inhibition reversed the protective effect of matrilin-3 on hemorrhagic transformation and infarction in the brains of ischemic rats

Given slight effects of matrilin exerting on the JNK signaling pathway, we therefore investigated whether the PI3K/AKT signaling pathway was implicated in the underlying mechanism of matrilin-3 in hemorrhagic transformation. In order to inhibit the PI3K/AKT signaling pathway, we treated rats with the PI3K inhibitor LY294002 ahead of tMCAO. Notably, a significant hemorrhage and increment of hemoglobin level were verified in the tMCAO+Matrilin-3 + LY294002 group, in contrast with those in the tMCAO+Matrilin-3 group (Fig. 2A, B, $p < 0.05$). As delineated in Fig. 2C, D, TTC staining validated that matrilin-3 overexpression greatly reduced the infarct volume in brains of ischemic rats ($p < 0.001$), but this effect was abrogated by LY294002 ($p < 0.01$).

Matrilin-3 was involved in the restoration of the BBB by activating the PI3K/AKT signaling pathway

From the rescue experiments of Western blot, LY294002 reduced protein expressions of p-PI3K/PI3K and p-AKT/AKT in the tMCAO+Matrilin-3 + LY294002 group, compared to the tMCAO+Matrilin-3 group (Fig. 3A–C, $p < 0.001$). ZO-1, VE-cadherin, and occludin acting as pivotal roles in endothelial cell integrity were found to be aberrantly expressed in the disruption of the BBB (31). As shown in Fig. 3D, E, ZO-1, VE-cadherin, and occludin protein expressions were downregulated in ischemic rat brains ($p < 0.001$),

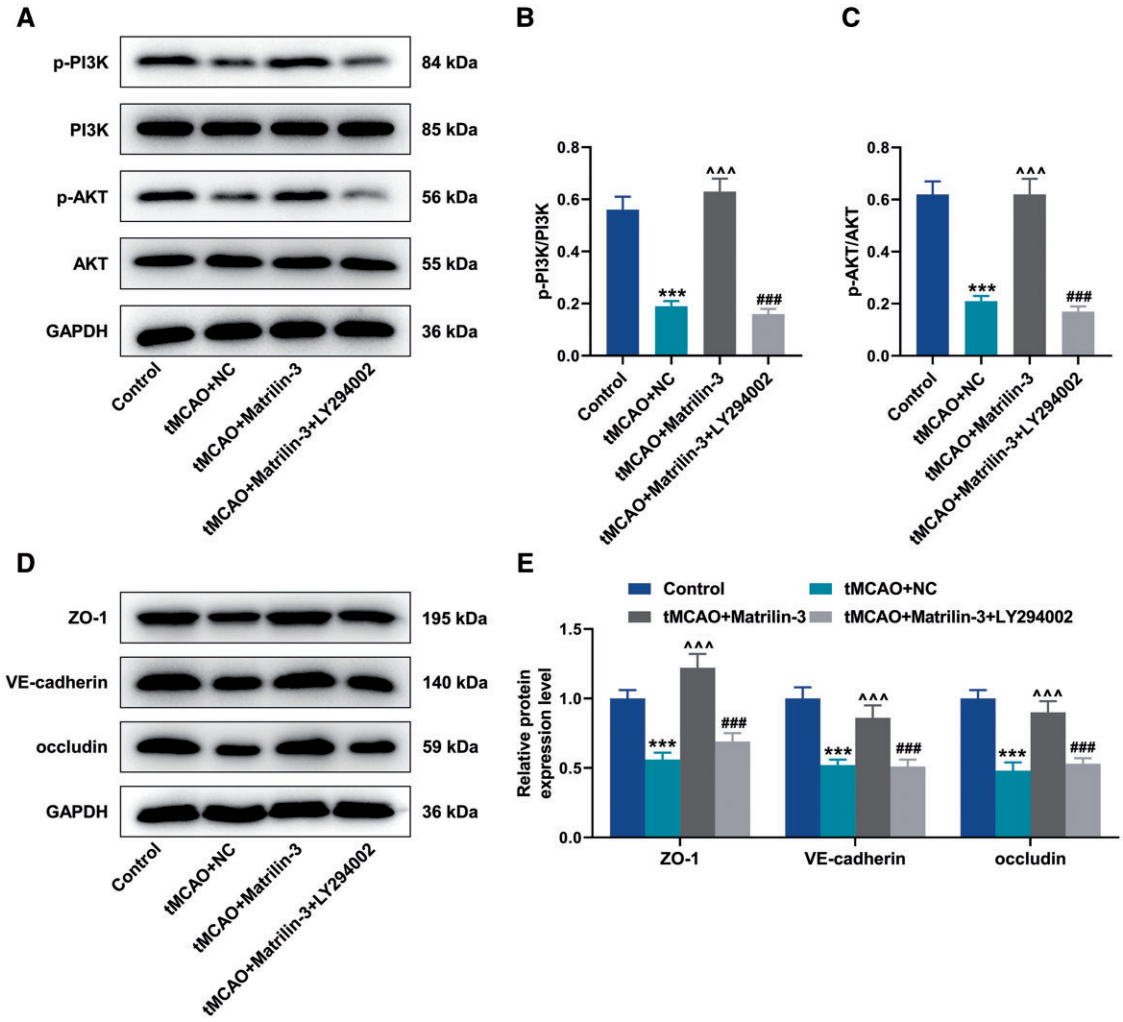

Figure 3. Matrilin-3 was involved in the restoration of the BBB via the PI3K/AKT signaling pathway. **(A–E)** Ischemic stroke modeling was performed on rats who were injected with or without adenovirus-mediated matrilin-3 plasmids and LY294002 (Control, tMCAO, tMCAO+NC, tMCAO+Matrilin-3, and tMCAO+Matrilin-3 + LY294002 groups). Western blot was used for quantitative analysis of p-PI3K/PI3K, p-AKT/AKT, ZO-1, VE-cadherin, and occludin protein expressions in each group. GAPDH served as the loading control. The data are presented as the mean±SD of 3 independent experiments; $^{***}p < 0.001$ versus Control; $^{\wedge\wedge\wedge}p < 0.001$ versus tMCAO+NC; $^{\#\#\#}p < 0.001$ versus tMCAO+Matrilin-3. Abbreviations: ZO-1, zonula occludens-1; VE-cadherin, vascular endothelial cadherin.

but these tendencies were reversed following matrilin-3 overexpression ($p < 0.001$). Compared with the tMCAO+Matrilin-3 group, LY294002 injection resulted in decreased expressions of ZO-1, VE-cadherin, and occludin in the tMCAO+Matrilin-3 + LY294002 group (Fig. 3D, E, $p < 0.001$). In addition, it was determined that the protein expression of YTHDF2 was higher in the brains of ischemic rats than that in the brains of normal rats (Fig. 4A, B, $p < 0.001$).

Oxygen-glucose deprivation-induced YTHDF2 upregulation and matrilin-3 downregulation in C8-D1A cells

To further verify the mechanism of matrilin-3 on regulating ischemic stroke, oxygen-glucose deprivation (OGD) subsequently was performed on C8-D1A cells for mimicking in vitro ischemic stroke. Compared with the cells in the glucose-free medium with normoxic condition, YTHDF2 expression was increased and matrilin-3 expression was decreased in the cells cultured with glucose-free medium in a hypoxic environment (Fig. 4C–E, $p < 0.01$).

YTHDF2 knockdown protected C8-D1A cells against OGD-induced injury by binding to matrilin-3

After transfection with shYTHDF2, the expression of YTHDF2 was significantly downregulated in C8-D1A cells (Fig. 5A, $p < 0.001$). In contrast to the cells transfected with scramble shRNA, shYTHDF2 elevated the expression of matrilin-3 in cells (Fig. 5B, $p < 0.001$). According to RNA immunoprecipitation (RIP) assay, the enrichment of matrilin-3 in the anti-YTHDF2-tagged immunoprecipitates from the cells transfected with shYTHDF2 (Fig. 5C, $p < 0.001$), indicating the binding of matrilin-3 and YTHDF2. Additionally, YTHDF2 knockdown reduced the decay of matrilin-3 in the

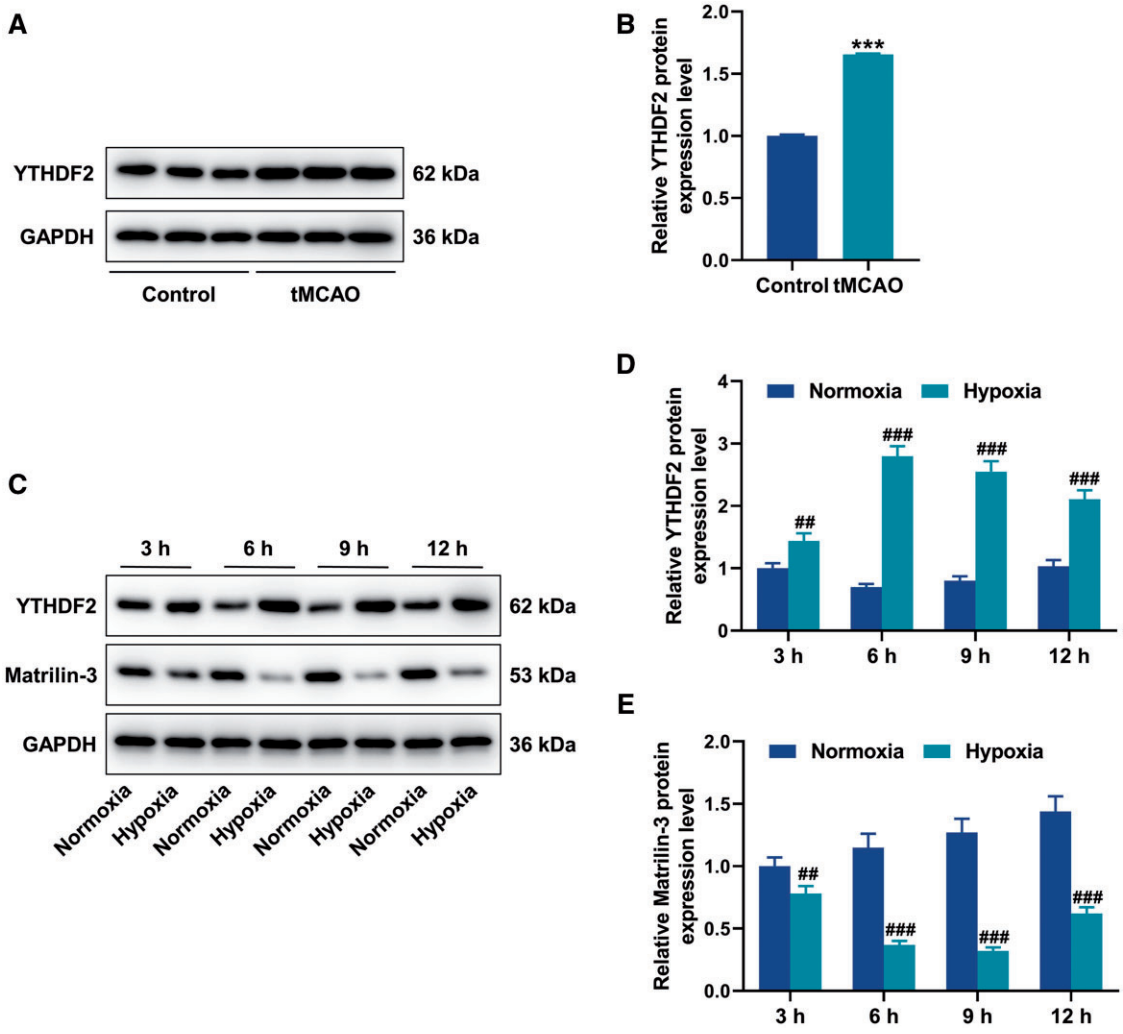

Figure 4. Expressions of YTHDF2 and matrilin-3 in C8-D1A cells after OGD. **(A, B)** Western blot was used to detect the protein expression of YTHDF2 in the brains of rats received with or without ischemic stroke modeling. **(C–E)** C8-D1A cells in glucose-free medium were induced by normoxia or hypoxia for 3, 6, 9, and 12 hours before subjected to Western blot for detecting YTHDF2 and matrilin-3 protein expressions. GAPDH served as the loading control. The data are presented as the mean±SD of 3 independent experiments; $^{***}p < 0.001$ versus Control; $^{\#\#}p < 0.01$, $^{\#\#\#}p < 0.001$ versus Normoxia. Abbreviation: YTHDF2, YTH N6-methyladenosine RNA binding protein F2.

ACTD-treated cells (Fig. 5D, $p < 0.01$). In C8-D1A cells, it was detected that OGD facilitated expressions of TNF-α and IL-6 (Fig. 5E, F, $p < 0.001$), but these effects were abrogated in the absence of YTHDF2 (Fig. 5E, F, $p < 0.001$). To validate YTHDF2 acting as a regulator for matrilin-3, we transfected shMatrilin-3 into C8-D1A cells to suppress the expression of matrilin-3 (Fig. 6A, $p < 0.001$). Of note, TNF-α and IL-6 expressions were increased in the cells transfected with shMatrilin-3 (Fig. 6B, C, $p < 0.001$), but these situations were rescued following YTHDF2 knockdown (Fig. 6B, C, $p < 0.001$). As demonstrated in Figure 6D–H, downregulation of matrilin-3 resulted in decreased protein expressions of p-PI3K/PI3K, p-AKT/AKT, ZO-1, VE-cadherin, and occludin in the cells ($p < 0.01$), whereas these effects were reversed by YTHDF2 knockdown ($p < 0.01$). Compared with the cells transfected with shYTHDF2 alone, the effects of YTHDF2 knockdown on inhibiting TNF-α and IL-6 expressions, as well as on promoting p-PI3K/PI3K, p-AKT/AKT, ZO-1, VE-cadherin, and occluding protein expressions were all reversed by matrilin-3 deficiency (Fig. 6B–H, $p < 0.001$).

DISCUSSION

The hemorrhagic transformation that accompanies endovascular treatment of patients with ischemic stroke, (particularly if symptomatic), is directly related to mortality and disability thereby posing a serious threat to stroke outcome. Thus, it is urgent to understand the mechanisms by which hemorrhagic transformation occurs.

Previous studies indicate that high levels of hemoglobin are strongly associated with thrombotic disorders such as ischemic stroke and myocardial infarction (32–34). Elevated hemoglobin levels increase blood viscosity and resistance to blood flow, which affects blood circulation, decreases oxygen supply

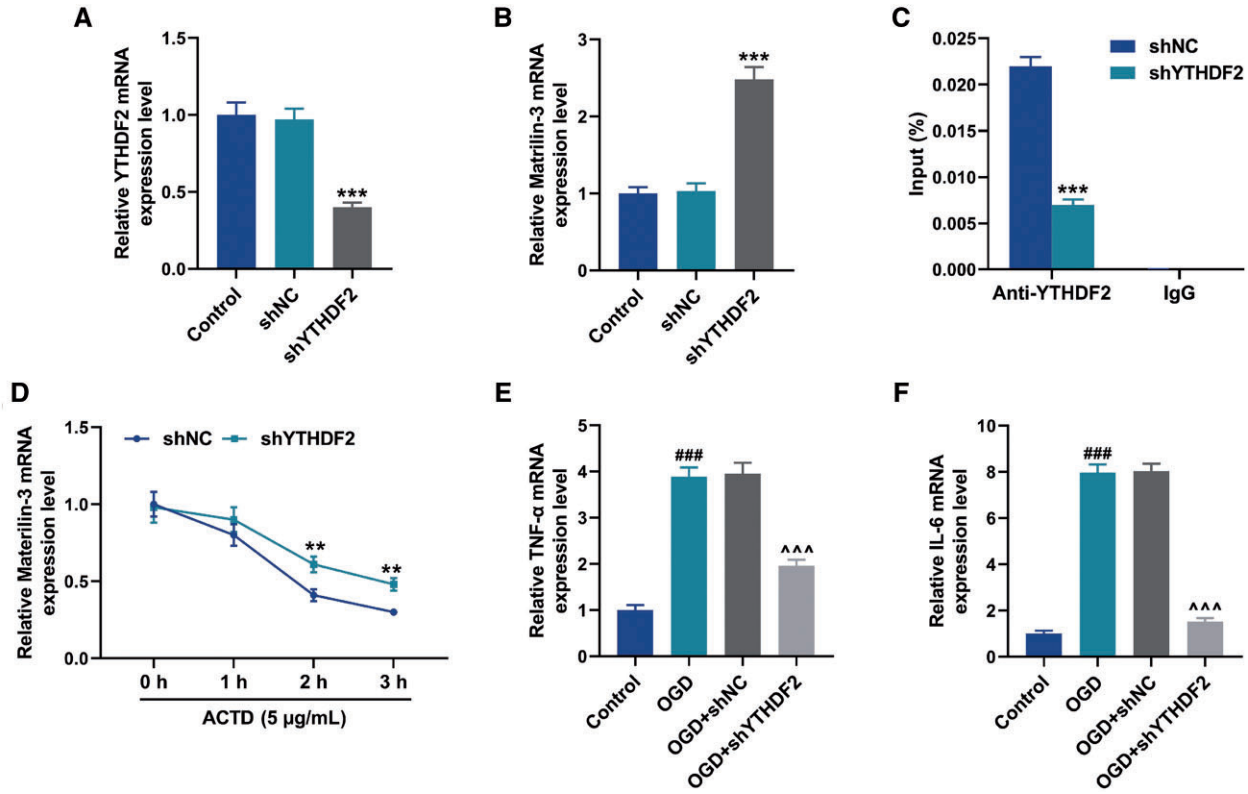

Figure 5. YTHDF2 bound to matrilin-3 and YTHDF2 knockdown reduced the inflammation of OGD-induced C8-D1A cells. **(A, B)** QRT-PCR was employed to detect YTHDF2 and matrilin-3 expressions in C8-D1A cells transfected with or without shNC/shYTHDF2. **(C)** RNA immunoprecipitation assay was performed to verify the binding of YTHDF2 and matrilin-3. **(D)** C8-D1A cells transfected with or without shNC/shYTHDF2 were subjected to 5 μg/mL ACTD treatment for 0, 1, 2, and 3 hours, followed by qRT-PCR for detecting the changes of matrilin-3 decay. **(E, F)** C8-D1A cells transfected with or without shNC/shYTHDF2 were subjected to hypoxic induction in glucose-free medium for obtaining OGD models (Control, OGD, OGD+shNC, and OGD+shYTHDF2 groups). TNF-α and IL-6 expressions in each group were determined using qRT-PCR. GAPDH served as the loading control. The data are presented as the mean± SD of 3 independent experiments; $^{**}p < 0.01$, $^{***}p < 0.001$ versus shNC; $^{\#\#\#}p < 0.001$ versus Control; $^{\wedge\wedge\wedge}p < 0.001$ versus OGD+shNC. Abbreviations: shYTHDF2, shRNA targeting YTHDF2; shNC, scramble shRNA; ACTD, Actinomycin D; OGD, oxygen-glucose deprivation; TNF-α, tumor necrosis factor alpha; IL-6, interleukin 6.

to the brain, and increases the risk of infarction in ischemic stroke areas. Chen et al (35) observed intracranial hemorrhage and elevated hemoglobin level in an ischemia-reperfusion brain injury model in rats. The present study revealed that matrilin-3 overexpression prominently reduced hemorrhage, hemoglobin content, and infarct volume in ischemic rat brains, implying that matrilin-3 may be used as a target to prevent hemorrhagic transformation during ischemic stroke.

When cerebral hemorrhage occurs, a series of secondary injuries develop within the brain tissue surrounding the hematoma, prompting apoptosis and necrosis of some neurons and exacerbating neurological dysfunction. For this reason, reducing apoptosis of neuronal cells after hemorrhage is key to alleviating brain injury, restoring cerebral function and inhibiting hemorrhagic transformation. Evidence has shown that the PI3K/AKT signaling pathway is one of the important pathways in the transduction of cerebral ischemia and apoptosis in the nervous system (36–38). PI3K, as a kinase involved in cell growth and skeletal remodeling, is an essential anti-apoptotic regulator (39). PI3K phosphorylation drives AKT activation which regulates apoptosis by promoting or inhibiting the expressions of its downstream target proteins such as Caspase 9, NF-κB, and mTOR (40). In tMCAO mice, Jin et al (31) demonstrated that the PI3K/AKT/GSK3β signaling pathway was activated in brain tissues after avenanthramide C treatment, which effectively impeded neuronal apoptosis. In addition, Vincourt et al (19) confirmed that matrilin-3 promoted integration of ECM in chondrocytes, which was positively correlated with AKT phosphorylation. In our study, the activation of PI3K/AKT pathway was revealed by Western blot in ischemic rat brains following matrilin-3 overexpression, but LY294002 rescued this situation. Besides, JNK signaling pathway is also involved in regulating cell apoptosis and is wildly studied in ischemic stroke. It has been confirmed that anti-apoptotic protein Bcl-2 was found to lose its apoptosis-inhibiting effect after JNK phosphorylation (41).

At the microvascular level, there is evidence that the main mechanism of hemorrhagic transformation is related to the enhanced permeability and disruption of BBB integrity. The BBB is a physiological barrier structure that exists between the

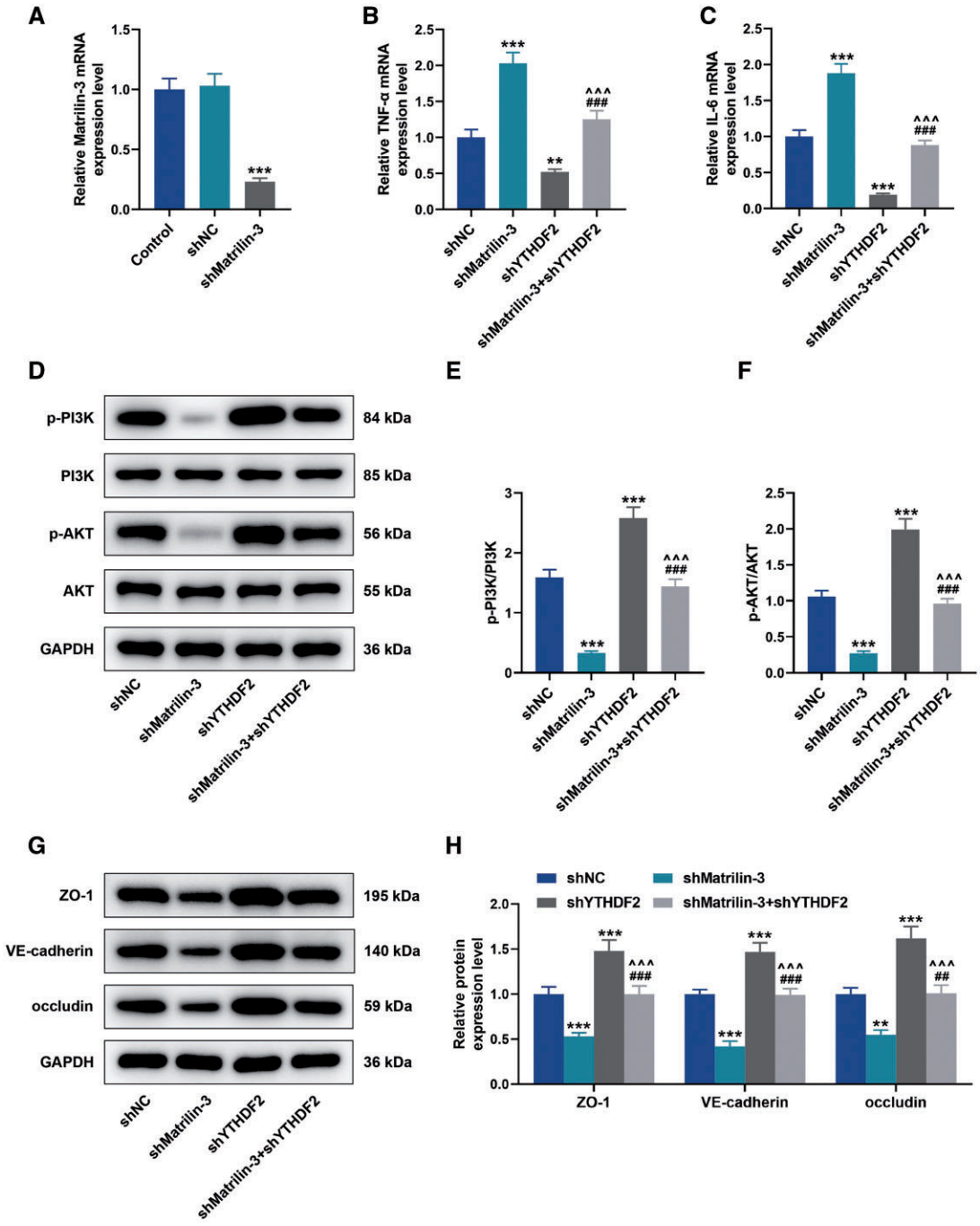

Figure 6. YTHDF2 knockdown suppressed inflammation, the PI3K/AKT signaling pathway and BBB-related proteins in C8-D1A cells by regulating matrilin-3. **(A)** QRT-PCR was employed to detect the expression of matrilin-3 in C8-D1A cells transfected with or without shNC/shMatrilin-3. **(B–C)** C8-D1A cells transfected with shMatrilin-3 or/and shYTHDF2 (Control, shMatrilin-3, shYTHDF2, and shMatrilin-3 + shYTHDF2 groups). TNF-α and IL-6 expressions in each group were determined using qRT-PCR. **(D–H)** Western blot was used for quantitative analysis of p-PI3K/PI3K, p-AKT/AKT, ZO-1, VE-cadherin, and occludin protein expressions in each group. GAPDH served as the loading control. The data are presented as the mean±SD of 3 independent experiments; $^{**}p < 0.01$, $^{***}p < 0.001$ versus shNC; $^{\#\#}p < 0.01$, $^{\#\#\#}p < 0.001$ versus shMatrilin-3; $^{\wedge\wedge\wedge}p < 0.001$ versus shYTHDF2. Abbreviation: shMatrilin-3, shRNA targeting matrilin-3.

blood circulation of the brain and neural tissue (42). It consists of cerebrovascular endothelial cells, astrocyte peduncles, pericytes, and basement membranes, each playing a critical role in maintaining the physiological homeostasis of the central nervous system (43). The study of Mark et al (44) reported that BBB permeability was increased by alteration of tight junctions after hypoxia-reoxygenation in the brain. In the composition of tight junction, occludin binds to adjacent cells through the extracellular portion of the cell membrane to produce paracellular closure, which plays a role in transmembrane

resistance of BBB and the formation of intercellular water channels (45). ZO-1 acts as a bridge in the connection between occludin and intracellular skeletal system, and in the signaling mechanism (46). VE-cadherin is predominantly found in vascular endothelial cells and is a key adhesion-linked protein that is closely associated with vascular permeability (47). In this study, we uncovered that matrilin-3 overexpression upregulated ZO-1, VE-cadherin, and occludin in ischemic rat brains, which were reversed by LY294002. It is indicated that matrilin-3 can improve the BBB in ischemic stroke to reduce the risk of intracranial hemorrhage through regulating the PI3K/AKT pathway.

Epigenetically, N6-methyladenosine (m^6A) methylation is the most common and reversible mRNA modification, and there is growing evidence that it plays a pivotal role in many pathological processes during ischemic stroke (48, 49). Thus, an in-depth understand of m^6A modification-mediated mechanisms underlying the pathogenesis of ischemic stroke is conducive to the development of therapeutic approaches for preventing and treating hemorrhagic transformation. Based on the analysis of GSE16561 and GSE22255 datasets, a recent study has reported 3 significantly upregulated m^6A regulators (IGF2BP2, IGF2BP1, YTHDF2) in patients with ischemic stroke (50); among them YTHDF2 is recognized as a reader and usually responsible for degrading mRNAs in a m^6A-independent manner (51). In the brains of ischemic rats, we determined the significant upregulation of YTHDF2. Intriguingly, matrilin-3 has been highlighted to exert protective effect on nucleus pulposus cells through exosome delivery-mediated intercellular crosstalk (52). Taking into consideration all the above, we hypothesize that matrilin-3 may be delivered to endothelial cells from astrocytes to promote BBB repair. As expected, we observed that OGD-induced YTHDF2 upregulation and matrilin-3 downregulation in C8-D1A cells, as well as following results of RIP assay and RNA decay assay demonstrated that YTHDF2 bound to matrilin-3 and negatively regulated the stability of matrilin-3. The study of Liu et al (53) recently has showed that astrocytes can protect human microvascular endothelial cells against hypoxia-caused injury and enhance BBB function. In our in vitro experiments, YTHDF2 knockdown was found to inhibit the release of TNF-α and IL-6, as well as promoted expression of BBB-related proteins and the activation of PI3K/AKT pathway in C8-D1A cells. Such effects of YTHDF2 knockdown were accomplished by stabilizing the expression of matrilin-3.

In conclusion, this study unveils the important role of matrilin-3 in attenuating the hemorrhagic transformation after ischemic stroke. Mechanistically, downregulation of YTHDF2 enhances the stability of matrilin-3 to promote BBB function repair via the PI3K/AKT pathway. These findings support matrilin-3 as a promising target for the treatment of stroke.

FUNDING

This study was funded by Zhejiang Provincial Natural Science Found (No. LY19H090016).

CONFLICT OF INTEREST

The authors have no duality or conflicts of interest to declare.

DATA AVAILABILITY

The analyzed data sets generated during the study are available from the corresponding author on reasonable request.

REFERENCES

1. Tsai CF, Anderson N, Thomas B, et al. Comparing risk factor profiles between intracerebral hemorrhage and ischemic stroke in Chinese and White populations: Systematic review and meta-analysis. PLoS One 2016;11:e0151743
2. Chen S, Lu X, Zhang W, et al. Does prior antiplatelet treatment increase the risk of hemorrhagic transformation and unfavorable outcome on day 90 after intravenous thrombolysis in acute ischemic stroke patients? J Stroke Cerebrovasc Dis 2016;25:1366–70
3. Amani H, Mostafavi E, Alebouyeh MR, et al. Would colloidal gold nanocarriers present an effective diagnosis or treatment for ischemic stroke? Int J Nanomedicine 2019;14:8013–8031
4. Momosaki R, Yasunaga H, Kakuda W, et al. Very early versus delayed rehabilitation for acute ischemic stroke patients with intravenous recombinant tissue plasminogen activator: A nationwide retrospective cohort study. Cerebrovasc Dis 2016;42:41–8
5. Roth C, Papanagiotou P, Behnke S, et al. Stent-assisted mechanical recanalization for treatment of acute intracerebral artery occlusions. Stroke 2010;41:2559–67
6. Goyal M, Menon BK, van Zwam WH, et al.; HERMES Collaborators. Endovascular thrombectomy after large-vessel ischaemic stroke: A meta-analysis of individual patient data from five randomised trials. Lancet 2016;387:1723–31
7. Ravindren J, Aguilar Pérez M, Hellstern V, et al. Predictors of outcome after endovascular thrombectomy in acute basilar artery occlusion and the 6hr time window to recanalization. Front Neurol 2019;10:923
8. Rosell A, Foerch C, Murata Y, et al. Mechanisms and markers for hemorrhagic transformation after stroke. Acta Neurochir Suppl 2008;105:173–8
9. Krizanac-Bengez L, Hossain M, Fazio V, et al. Loss of flow induces leukocyte-mediated MMP/TIMP imbalance in dynamic in vitro blood-brain barrier model: Role of pro-inflammatory cytokines. Am J Physiol Cell Physiol 2006;291:C740–9
10. Heras-Sandoval D, Pérez-Rojas JM, Hernández-Damián J, et al. The role of PI3K/AKT/mTOR pathway in the modulation of autophagy and the clearance of protein aggregates in neurodegeneration. Cell Signal 2014;26:2694–701
11. Kim JE, Kang TC. TRPC3- and ET(B) receptor-mediated PI3K/AKT activation induces vasogenic edema formation following status epilepticus. Brain Res 2017;1672:58–64
12. Lu H, Zhang LH, Yang L, et al. The PI3K/Akt/FOXO3a pathway regulates regeneration following spinal cord injury in adult rats through TNF-α and p27kip1 expression. Int J Mol Med 2018;41:2832–2838
13. Fan W, Li X, Huang L, et al. S-oxiracetam ameliorates ischemic stroke induced neuronal apoptosis through up-regulating α7 nAChR and PI3K/Akt/GSK3β signal pathway in rats. Neurochem Int 2018;115:50–60
14. Klatt AR, Becker AK, Neacsu CD, et al. The matrilins: Modulators of extracellular matrix assembly. Int J Biochem Cell Biol 2011;43:320–30
15. Korpos É, Deák F, Kiss I. Matrilin-2, an extracellular adaptor protein, is needed for the regeneration of muscle, nerve and other tissues. Neural Regen Res 2015;10:866–9
16. Wierer M, Prestel M, Schiller HB, et al. Compartment-resolved proteomic analysis of mouse aorta during atherosclerotic plaque

formation reveals osteoclast-specific protein expression. Mol Cell Proteomics 2018;17:321–334
17. Sozmen EG, DiTullio DJ, Rosenzweig S, et al. White matter stroke induces a unique oligo-astrocyte niche that inhibits recovery. J Neurosci 2019;39:9343–9359
18. Hillary RF, McCartney DL, Harris SE, et al. Genome and epigenome wide studies of neurological protein biomarkers in the Lothian Birth Cohort 1936. Nat Comm 2019;10:3160
19. Vincourt JB, Etienne S, Grossin L, et al. Matrilin-3 switches from anti- to pro-anabolic upon integration to the extracellular matrix. Matrix Biol 2012;31:290–8
20. Lu XD, Liu YR, Zhang ZY. Matrilin-3 alleviates extracellular matrix degradation of nucleus pulposus cells via induction of IL-1 receptor antagonist. Eur Rev Med Pharmacol Sci 2020;24:5231–5241
21. Muttigi MS, Kim BJ, Choi B, et al. Matrilin-3 codelivery with adipose-derived mesenchymal stem cells promotes articular cartilage regeneration in a rat osteochondral defect model. J Tissue Eng Regen Med 2018;12:667–675
22. Feng C, Wan H, Zhang Y, et al. Neuroprotective effect of danhong injection on cerebral ischemia-reperfusion injury in rats by activation of the PI3K-Akt pathway. Front Pharmacol 2020;11:298
23. Yao T, Ying X, Zhao Y, et al. Vitamin D receptor activation protects against myocardial reperfusion injury through inhibition of apoptosis and modulation of autophagy. Antioxid Redox Signal 2015;22:633–50
24. Zhang D, Jin W, Liu H, et al. ENT1 inhibition attenuates apoptosis by activation of cAMP/pCREB/Bcl2 pathway after MCAO in rats. Exp Neurol 2020;331:113362
25. Hernandes MS, Lassègue B, Hilenski LL, et al. Polymerase delta-interacting protein 2 deficiency protects against blood-brain barrier permeability in the ischemic brain. J Neuroinflammation 2018;15:45
26. Huang CS, Zhu YQ, Xu QC, et al. YTHDF2 promotes intrahepatic cholangiocarcinoma progression and desensitises cisplatin treatment by increasing CDKN1B mRNA degradation. Clin Transl Med 2022;12:e848
27. Livak KJ, Schmittgen TD. Analysis of relative gene expression data using real-time quantitative PCR and the 2(-Delta C(T)) Method. Methods 2001;25:402–8
28. Chen J, Yang L, Geng L, et al. Inhibition of Acyl-CoA synthetase long-chain family member 4 facilitates neurological recovery after stroke by regulation ferroptosis. Front Cell Neurosci 2021;15:632354
29. Hirano S. Western blot analysis. Methods in Molecular Biology (Clifton, NJ) 2012;926:87–97
30. Luo J, Peng S, Bai W, et al. Matrilin-2 prevents the TNFα-induced apoptosis of WB-F344 cells via suppressing JNK pathway. Biotechnol Appl Biochem 2019;66:309–315
31. Jin B, Kim H, Choi JI, et al. Avenanthramide C prevents neuronal apoptosis via PI3K/Akt/GSK3β signaling pathway following middle cerebral artery occlusion. Brain Sci 2020;10:878
32. Yotsueda R, Tanaka S, Taniguchi M, et al. Hemoglobin concentration and the risk of hemorrhagic and ischemic stroke in patients undergoing hemodialysis: The Q-cohort study. Nephrol Dial Transplant 2018;33:856–864
33. Jadczyk T, Baranski K, Syzdol M, et al. Bioactive sphingolipids, complement cascade, and free hemoglobin levels in stable coronary artery disease and acute myocardial infarction. Mediators Inflamm 2018;2018:2691934
34. Thom CS, Dickson CF, Gell DA, et al. Hemoglobin variants: Biochemical properties and clinical correlates. Cold Spring Harb Perspect Med 2013;3:a011858
35. Chen HS, Chen XM, Feng JH, et al. Peroxynitrite decomposition catalyst reduces delayed thrombolysis-induced hemorrhagic transformation in ischemia-reperfused rat brains. CNS Neurosci Ther 2015;21:585–90
36. Wang C, Wei Z, Jiang G, et al. Neuroprotective mechanisms of miR-124 activating PI3K/Akt signaling pathway in ischemic stroke. Exp Ther Med 2017;13:3315–3318
37. Jin XF, Wang S, Shen M, et al. Effects of rehabilitation training on apoptosis of nerve cells and the recovery of neural and motor functions in rats with ischemic stroke through the PI3K/Akt and Nrf2/ARE signaling pathways. Brain Res Bull 2017;134:236–245
38. Tu XK, Zhang HB, Shi SS, et al. 5-LOX inhibitor zileuton reduces inflammatory reaction and ischemic brain damage through the activation of PI3K/Akt signaling pathway. Neurochem Res 2016;41:2779–2787
39. Yao R, Cooper GM. Requirement for phosphatidylinositol-3 kinase in the prevention of apoptosis by nerve growth factor. Science 1995;267:2003–6
40. Arslan F, Lai RC, Smeets MB, et al. Mesenchymal stem cell-derived exosomes increase ATP levels, decrease oxidative stress and activate PI3K/Akt pathway to enhance myocardial viability and prevent adverse remodeling after myocardial ischemia/reperfusion injury. Stem Cell Res 2013;10:301–12
41. Maundrell K, Antonsson B, Magnenat E, et al. Bcl-2 undergoes phosphorylation by c-Jun N-terminal kinase/stress-activated protein kinases in the presence of the constitutively active GTP-binding protein Rac1. J Biol Chem 1997;272:25238–42
42. Hamann GF, Okada Y, del Zoppo GJ. Hemorrhagic transformation and microvascular integrity during focal cerebral ischemia/reperfusion. J Cereb Blood Flow Metab 1996;16:1373–8
43. Daneman R, Prat A. The blood-brain barrier. Cold Spring Harb Perspect Biol 2015;7:a020412
44. Mark KS, Davis TP. Cerebral microvascular changes in permeability and tight junctions induced by hypoxia-reoxygenation. Am J Physiol Heart Circ Physiol 2002;282:H1485–94
45. Li JY, Boado RJ, Pardridge WM. Blood-brain barrier genomics. J Cereb Blood Flow Metab 2001;21:61–8
46. Wolburg H, Lippoldt A. Tight junctions of the blood-brain barrier: Development, composition and regulation. Vascul Pharmacol 2002;38:323–37
47. Li W, Chen Z, Chin I, et al. The role of VE-cadherin in blood-brain barrier integrity under central nervous system pathological conditions. Curr Neuropharmacol 2018;16:1375–1384
48. Zhu R, Tian D, Zhao Y, et al. Genome-wide detection of m(6)A-associated genetic polymorphisms associated with ischemic stroke. J Mol Neurosci 2021;71:2107–2115
49. Chang H, Yang J, Wang Q, et al. Role of N6-methyladenosine modification in pathogenesis of ischemic stroke. Expert Rev Mol Diagn 2022;22:295–303
50. Tao H, Dong L, Li L. N6-methyladenosine modulation classes and immune microenvironment regulation in ischemic stroke. Front Mol Neurosci 2022;15:1013076
51. Li J, Xie H, Ying Y, et al. YTHDF2 mediates the mRNA degradation of the tumor suppressors to induce AKT phosphorylation in N6-methyladenosine-dependent way in prostate cancer. Mol Cancer 2020;19:152
52. Guo Z, Su W, Zhou R, et al. Exosomal MATN3 of urine-derived stem cells ameliorates intervertebral disc degeneration by antisenescence effects and promotes NPC proliferation and ECM synthesis by activating TGF-β. Oxid Med Cell Longev 2021;2021:5542241
53. Liu J, Li J. Astrocytes protect human brain microvascular endothelial cells from hypoxia injury by regulating VEGF expression. J Healthc Eng 2022;2022:1884959